Hindawi
Mathematical Problems in Engineering
Volume 2019, Article ID 7453602, 10 pages
https://doi.org/10.1155/2019/7453602

Research Article

A Composite Guidance Law for Suppressing Measurement Noise of LOS Angular Rate

Feng Chen,[1] **Guangjun He**,[1] **and Qifang He**[2]

[1]*Air and Missile Defense College, Air Force Engineering University, Xi'an 710051, China*
[2]*Information and Navigation College, Air Force Engineering University, Xi'an 710077, China*

Correspondence should be addressed to Feng Chen; 1904812819@qq.com

Received 17 September 2018; Accepted 8 November 2018; Published 6 January 2019

Academic Editor: Jorge Rivera

To effectively intercept a low-altitude target in clutter background, a nonsingular fast terminal sliding mode guidance law is designed. The designed guidance law can fully exploit the fast convergence characteristics of linear sliding mode control and the finite-time-convergent characteristics of terminal sliding mode control to ensure that the line-of-sight (LOS) angle converges to a desired angle in a limited time at a faster rate. Utilizing the smooth switching characteristics of the hyperbolic tangent function similar to the saturation function, a finite-time-convergent differentiator is designed. Meanwhile, a new finite-time-convergent disturbance observer designed on the tracking differentiator can effectively track the ideal LOS angular rate, suppress the measurement noise, and make a smooth estimation of the target maneuvering acceleration in clutter background. Combining the estimated value of the disturbance observer, the sign function with switch coefficient is introduced to design a composite nonsingular fast terminal sliding mode guidance law. The simulation results show that the composite guidance law can not only effectively suppress the measurement noise of the LOS angular rate and improve the accuracy of low-altitude target intercepting, but also greatly reduce the energy consumption in the interception process.

1. Introduction

Interception of a low-altitude target has always been a worldwide challenge in the field of air defense. First of all, in order to improve the performance of the low-altitude target detecting and tracking, it is usually required that the line-of-sight (LOS) angle between the interceptor and the target satisfies a specific angle constraint [1–3]. Secondly, influenced by earth curvature and ground or sea clutter, low-altitude targets are difficult to detect and discover [4], which greatly shortens the time for air defense early warning. Therefore, fast response characteristics of the interceptor guidance system are required. Finally, the radar seeker's measurement of the LOS angular rate is susceptible to the multipath effect of the ground or sea surface, resulting in the measurement noise and the great reduction of the guidance accuracy [5]. Although the attack angle can be restricted by the improved proportional navigation (PN) guidance law, the accuracy of intercepting maneuvering targets will be greatly reduced [6]. Bardhan and Ghose designed a differential game guidance law to meet the angle constraint for maneuvering targets [7]. Yu et al. designed an optimal guidance law, which can satisfy the terminal angle constraint based on the principle of the most fuel-saving [8]. However, the guidance laws mentioned above are of poor anti-interference performance and cannot effectively intercept the low-altitude target in the clutter background. Sliding mode control is widely studied because of its good robustness and antijamming performance [9, 10], whereas the general linear sliding mode (LSM) control only has gradual convergence properties [11]. To solve this problem, Skruch proposed a terminal sliding mode (TSM) control with finite-time-convergent characteristics [12]. But there are still two inherent disadvantages in TSM control: firstly, the singularity problem is easily produced; secondly, the convergence rate of the system state is slower than that of general LSM control. In order to solve the singularity problem, nonsingular terminal sliding mode (NTSM) control is proposed by Cho et al. [13]. What is more, a fast terminal sliding mode (FTSM) control was proposed by Boonsatit and Pukdeboon to solve the problem of slow convergence rate

[14]. However, these two kinds of TSM control cannot solve the above two problems at the same time.

The radar seeker of an interceptor is susceptible to the ground clutter and multipath effects when detecting and tracking the low-altitude target, and measurement noise is easily generated. Current researches on seeker's measurement noise mainly focus on three aspects, that is, filtering [15], measurement model [16], and noise estimation [17]. However, the seeker is only regarded as an independent measurement system in the above methods, and the influence of seeker's measurement noise of the whole interception system is not considered. Meanwhile, the influence of measurement noise on the energy consumption during the whole interception process is also neglected. Due to the influence of ground clutter, the maneuvering acceleration of the low-altitude target is difficult to accurate obtained in practice. In most literatures, maneuvering acceleration of the target is usually regarded as an uncertain disturbance, and then a nonlinear disturbance observer (NDO) will be designed to estimate the acceleration of the target. An NDO is designed by Zhen under the premise that the unknown disturbance is a slow variable and its first derivative is zero, but it is too conservative [18]. Xu et al. designed a new NDO on the assumption that the derivative of the disturbance is bounded, which is of limited engineering practicality [19]. Han et al. designed a disturbance observer based on fault estimation [20]. It does not require any information about the disturbance in advance and has broader application prospects, but effective suppression of the measurement noise of the input signal cannot be achieved. To solve the problem, a new tracking differentiator (TD) was designed by Qi et al. It has a good performance to suppress the noise of the input signal, but the first derivative of the input signal is of limited estimation accuracy [21].

The remainder of this paper is organized as follows. In Section 2, a nonsingular fast terminal sliding mode (NFTSM) guidance law is designed, which has both the finite-time-convergent characteristics of TSM control and the fast response characteristics of LSM control. In Section 3, a finite-time-convergent differentiator (FCD) is designed by introducing a hyperbolic tangent function. Meanwhile, to track the ideal LOS angular rate and estimate the target acceleration in the clutter background, a finite-time-convergent disturbance observer (FCDO) is designed based on the FCD. In Section 4, a composite nonsingular fast terminal sliding mode (CNFTSM) guidance law is designed by introducing the estimated value of the FCDO and the sign function with switch coefficient into the NFTSM guidance law. In Section 5, simulation results to demonstrate the excellent tracking performance of the FCD and the excellent interception performance of the proposed CNFTSM guidance law are shown. Finally, conclusions are drawn in Section 6.

2. Interception Model for Low-Altitude Targets

An interceptor usually performs a dive attack on the target from a high altitude when intercepting a low-altitude target, in order to enlarge the vision range of the radar seeker for target detection. To design an interception trajectory that satisfies the specific LOS angle constraint, only the interception situation of the longitudinal plane is analyzed. The interceptor as well as the target is regarded as a mass point, and the engagement geometry of the interceptor and the target is shown in Figure 1 [22].

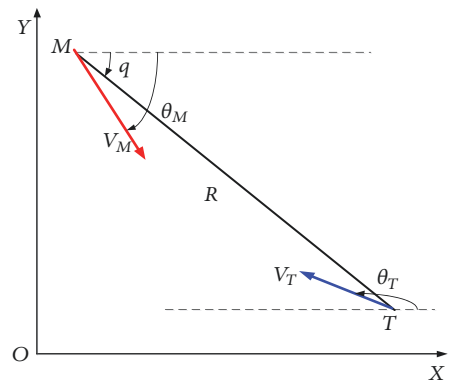

Figure 1: Interception model for low-altitude targets.

Assume that the velocity of the interceptor and the target are both constant, and the relative motion equation of the interceptor and the target can be described as

$$\dot{R} = -V_M \cos \eta_M + V_T \cos \eta_T \tag{1}$$

$$R\dot{q} = V_M \sin \eta_M - V_T \sin \eta_T \tag{2}$$

$$\dot{\theta}_M = \frac{A_M}{V_M} \tag{3}$$

$$\dot{\theta}_T = \frac{A_T}{V_T}, \tag{4}$$

where $\eta_M = q - \theta_M$, $\eta_T = q - \theta_T$; V_M and V_T denote velocity of the interceptor and the target, respectively. θ_M and θ_T denote the flight path angle of the interceptor and the target, respectively. $\dot{\theta}_M$ and $\dot{\theta}_T$ denote the flight path angular rates of the interceptor and target, respectively. The relative range and the range rate between the interceptor and the target are denoted by R and $\dot{R}$. A_M and A_T are the acceleration commands of the interceptor and the target, respectively. q and $\dot{q}$ denote the LOS angle and the LOS angular rate, respectively. Let all angles of the counterclockwise direction be positive.

Differentiate (2) with respect to time and substitute it into (1), (3), and (4), which yields

$$\ddot{q} = \frac{-2\dot{R}\dot{q}}{R} + \frac{A_{Tq}}{R} - \frac{A_{Mq}}{R}, \tag{5}$$

where $A_{Tq} = A_T \cos \eta_T$; $A_{Mq} = A_M \cos \eta_M$.

3. NFTSM Guidance Law Design

Lemma 1 (see [23]). *Supposing that $V(t)$ is defined as a smooth positive function on C^1 and satisfies $\dot{V}(t) + \beta_1 V(t) + \beta_2 V(t)^\gamma \leq 0$ for $\beta_1, \beta_2 > 0$ and $\gamma \in (0, 1)$, then there exists*

an area $U_0 \subset \mathbf{R}^n$ and any $V(t)$ which starts from the area can reach $V(t) \equiv 0$ in finite time.

$$T_{reach} \leq t_0 + \frac{1}{\beta_1 (1-\gamma)} \ln \frac{\beta_1 V^{1-\gamma}(t_0) + \beta_2}{\beta_2}, \quad (6)$$

where $V(t_0)$ is the initial value of $V(t)$; t_0 is the initial time.

In order to more effectively detect and track the target, the LOS angle must be constrained to a specific angle when intercepting a low-altitude target. Meanwhile, the LOS angular rate must converge to near zero to reduce the miss distance. Therefore, the state variables can be selected as

$$\begin{aligned} x_1 &= q - q_d \\ x_2 &= \dot{q} = \dot{x}_1, \end{aligned} \quad (7)$$

where q_d is the desired LOS angle.

Combining (5) and (7), it can be obtained that

$$\dot{x}_2 = f(x_1, x_2) + g(x_1, x_2) A_M + d, \quad (8)$$

where $f(x_1, x_2) = -2\dot{R}x_2/R$, $g(x_1, x_2) = \cos(x_1 + q_d - \theta_M)/R$, and $d = A_{Tq}/R$.

The purpose of the guidance law design is to constrain the state variables to zero as much as possible. In order to ensure that the state of the system can be converged to the equilibrium point $x_1 = x_2 = 0$ in a limited time with a fast convergence rate, the NFTSM surface can be selected as

$$S = x_2 + h_1 x_1 + h_2 g(x_1), \quad (9)$$

where $h_1, h_2 > 0$ and $g(x_1)$ is defined as

$$g(x_1) = \begin{cases} sig(x_1)^{\alpha} & |x_1| > \xi \\ m_1 x_1 + m_2 \operatorname{sign}(x_1) x_1^2 & |x_1| \leq \xi, \end{cases} \quad (10)$$

where $sig(x_1)^{\alpha} = |x_1|^{\alpha}\operatorname{sign}(x_1)$, $m_1 = (2-\alpha)\xi^{\alpha-1}$, $m_2 = (\alpha - 1)\xi^{\alpha-2}$, $0 < \alpha < 1$, and ξ is a small positive constant.

The sliding surface designed as (9) is composed of the linear term $h_1 x_1$ and the nonlinear term $h_2 g(x_1)$, which can fully exploit the fast convergence characteristics of LSM control and the finite-time-convergent characteristics of TSM control by choosing appropriate parameters h_1 and h_2.

Differentiating (9) with respect to time and substituting (8) into it yields

$$\dot{S} = \frac{-2\dot{R}x_2}{R} + \frac{A_{Tq}}{R} - \frac{A_{Mq}}{R} + h_1 x_2 + h_2 \dot{g}(x_1), \quad (11)$$

where

$$\dot{g}(x_1) = \begin{cases} \alpha |x_1|^{\alpha-1} x_2 & |x_1| > \xi \\ m_1 x_2 + 2m_2 \operatorname{sign}(x_1) x_1 x_2 & |x_1| \leq \xi. \end{cases} \quad (12)$$

From (12) we can see that the singular problem can be effectively avoided by NFTSM surface design when $x_1 = 0$. In order to further improve the convergence rate of the system, the approaching law of sliding mode is designed as

$$\dot{S} = -k_1 S - k_2 sig(S)^{\alpha_1}, \quad (13)$$

where $k_1, k_2 > 0$ and $0 < \alpha_1 < 1$.

Combine (11) and (13) to obtain the NFTSM guidance law as follows:

$$A_M = \frac{-2\dot{R}x_2 + A_{Tq} + R(h_1 x_2 + h_2 \dot{g}(x_1) + k_1 S + k_2 sig(S)^{\alpha_1})}{\cos(q - \theta_M)}. \quad (14)$$

When the guidance law shown as (14) is applied to intercepting the low-altitude target, it is necessary to measure the LOS angular rate x_2 and the target's maneuvering acceleration A_{Tq} in high accuracy. However, in the actual clutter background, the measurement value of the LOS angular rate may be disturbed by the multipath effect, and the accompanying measurement noise will further cause the general disturbance observer failing in effective estimation of the target's maneuvering acceleration. Therefore, a new type of disturbance observer needs to be designed, which can not only suppress the measurement noise of the LOS angular rate, but also accurately estimate the acceleration of the target. Following comes the designed FCDO.

4. FCDO Design

4.1. FCD Design. If noise of the input signal is regarded as a type of high-frequency chattering, inspired by the saturation function sat(·) that can reduce the chattering phenomenon, the differentiator can be constructed with a saturation function to suppress high-frequency chattering of the output, i.e., the differentiator can be insensitive to noise. The hyperbolic tangent function tanh(·) has better smooth switching characteristics near the zero point than the saturation function, therefore, measurement noise can be more effectively suppressed.

Combining with the hyperbolic tangent function, a new FCD is designed as follows:

$$\begin{aligned} \dot{z}_1 &= z_2 \\ \dot{z}_2 &= \lambda^n \left[-c_1 \tanh(z_1 - v(t)) - c_2 \tanh\left(\frac{z_2}{\lambda}\right) \right], \end{aligned} \quad (15)$$

where $\lambda, c_1, c_2 \in \mathbf{R}^+$ are parameters to be designed; $z_1, z_2 \in \mathbf{R}$ are the state variables; $v(t)$ is an input signal with measurement noise; z_1 is a tracking value of $v(t)$ after filtering out the measurement noise and z_2 is an estimated value of the first derivative of $v(t)$.

Theorem 2. *For system (15), there exist constants $\phi > 0$ and $\tau\phi > 2$ that make*

$$z_i - v^{(i-1)}(t) = O\left(\left(\frac{1}{\lambda}\right)^{\tau\phi - i + 1}\right), \quad i = 1, 2, \quad (16)$$

where $O((1/\lambda)^{\tau\phi-i+1})$ represents the approximation degree between z_i and $v^{(i-1)}(t)$; $\phi = (1-\vartheta)/\vartheta$ and $\vartheta \in (0, \min\{\tau/(\tau+2), 1/2\})$.

Proof. Consider the following second-order system:

$$\begin{aligned}\dot{z}_1 &= z_2\\ \dot{z}_2 &= f(z_1, z_2)\\ &= -c_1 \tanh(z_1) - c_2 \tanh(z_2),\end{aligned} \tag{17}$$

where $f(\cdot)$ is a continuous function and $f(0,0) = 0$.

Let $0 < z_1 < z_2$, and the Lyapunov function is selected as follows:

$$V = \int_0^{z_1} c_1 \tanh(\tau)\, d\tau + z_2^2 + 1. \tag{18}$$

Differentiating (18) with respect to time and then substituting (17) into it yield

$$\begin{aligned}\dot{V} &= c_1 \tanh(z_1)\dot{z}_1 + 2z_2\dot{z}_2\\ &= c_1 \tanh(z_1)\dot{z}_1 + 2z_2\left(-c_1 \tanh(z_1) - c_2 \tanh(z_2)\right)\\ &\le -c_1 \tanh(z_1) z_2\\ &\le -c_1 \tanh(z_1) z_1.\end{aligned} \tag{19}$$

According to the Lagrangian mean value theorem, there must be a variable $\eta_1 \in [0, z_1]$, which satisfies

$$\int_0^{z_1} c_1 \tanh(\tau)\, d\tau = c_1 z_1 \tanh(\eta_1) \le c_1 z_1 \tanh(z_1). \tag{20}$$

According to (20), (19) can be rewritten as

$$\dot{V} \le -\int_0^{z_1} c_1 \tanh(\tau)\, d\tau = -V + \Omega, \tag{21}$$

where $\Omega = z_2^2 + 1$.

Let

$$-V + \Omega = -V^\theta, \tag{22}$$

where $\theta > 0$.

Equation (22) can be rewritten into the form as follows:

$$V^\theta = V - \Omega < V. \tag{23}$$

According to $V > 1$ and $V^\theta < V$, it can be concluded that $0 < \theta < 1$. Combine (21) and (22) to obtain that

$$\dot{V} + V^\theta \le 0, \quad \theta \in (0,1). \tag{24}$$

Therefore, it can be seen that system (17) satisfies Assumption 1 in [24].

$\forall z \ne y \in \mathbf{R}$, it can be obviously obtained that

$$\begin{aligned}\left|\lim_{z\to y} \frac{\tanh(z) - \tanh(y)}{z - y}\right| &= \left|\frac{d[\tanh(z)]}{dz}\right|\\ &= \frac{1}{\cosh^2(z)} \le 1\end{aligned} \tag{25}$$

which implies

$$\left|\tanh(z) - \tanh(y)\right| \le \left|z - y\right|. \tag{26}$$

Therefore, Assumption 2 in [24] is set up.

Combine (17) and (26) to obtain that

$$\begin{aligned}&\left|f(\widetilde{z}_1, \widetilde{z}_2) - f(\overline{z}_1, \overline{z}_2)\right|\\ &\quad= \left|\left[c_1 \tanh(\overline{z}_1) - c_1 \tanh(\widetilde{z}_1)\right]\right.\\ &\quad\left.+ \left[c_2 \tanh(\overline{z}_2) - c_2 \tanh(\widetilde{z}_2)\right]\right| \le c_1\left|\overline{z}_1 - \widetilde{z}_1\right|\\ &\quad+ c_2\left|\overline{z}_2 - \widetilde{z}_2\right| \le \overline{d}\sum_{i=1}^{2}\left|\overline{z}_i - \widetilde{z}_i\right|,\end{aligned} \tag{27}$$

where $\overline{d} = \max\{c_1, c_2\}$.

Therefore, Assumption 3 in [24] is set up. And Theorem 2 is established if the input signal satisfies Assumption 4 in [24]. □

From (16), it can be seen that the estimation error is the high-order infinitesimal of $(1/\lambda)^{\tau\phi - i + 1}$. By selecting a sufficiently large design parameter λ, the estimation error can be arbitrarily small.

4.2. FCDO Designed Based on FCD. Based on the new FCD, then a new FCDO is designed to estimate the uncertain disturbance d in (8).

$$\begin{aligned}\dot{\hat{x}}_2 &= f(x_1, x_2) + g(x_1, x_2) A_M + \hat{d}\\ \dot{\hat{d}} &= \lambda^2\left[-c_1 \tanh(\hat{x}_2 - x_2) - c_2 \tanh\left(\frac{\hat{d}}{\lambda}\right)\right],\end{aligned} \tag{28}$$

where $\hat{x}_2$ and $\hat{d}$ are the estimated values of x_2 and d, respectively.

Theorem 3. *For system (28), if $\lambda \longrightarrow \infty$, then $\hat{x}_2 \longrightarrow x_2$, $\hat{d} \longrightarrow d$.*

Proof. Two cases are discussed as follows:

(1) If $\hat{x}_2 - x_2 = 0$, compare the first formula in (8) with that in (28) to get $\hat{d} - d = 0$. Thus, Theorem 3 is established

(2) If $\hat{x}_2 - x_2 \ne 0$, due to $\lambda \longrightarrow +\infty$, then $\tanh(\hat{d}/\lambda) \longrightarrow 0$; it can be obtained that

$$-c_1 \tanh(\hat{x}_2 - x_2) - c_2 \tanh\left(\frac{\hat{d}}{\lambda}\right) \ne 0 \tag{29}$$

which implies that

$$\left|\dot{\hat{d}}\right| = \lambda^2\left|-c_1 \tanh(\hat{x}_2 - x_2) - c_2 \tanh\left(\frac{\hat{d}}{\lambda}\right)\right| \longrightarrow +\infty. \tag{30}$$

That is to say, $\hat{d}$ is a fast variable relative to $f(x_1, x_2) + g(x_1, x_2)A_M$, and thus

$$\lim_{\lambda \longrightarrow +\infty} \frac{\mathrm{d}\left[f(x_1, x_2) + g(x_1, x_2) A_M + \hat{d}\right]}{\mathrm{d}t} = \dot{\hat{d}}$$
$$\lim_{\lambda \longrightarrow +\infty} \frac{f(x_1, x_2) + g(x_1, x_2) A_M + \hat{d}}{\lambda} = \frac{\hat{d}}{\lambda} \tag{31}$$

Right now, if the variable z_2 in (15) is replaced by $f(x_1, x_2) + g(x_1, x_2)A_M + \hat{d}$ and combined with (31), (28) can be obtained; i.e., (28) is a special form of (15). Then, similar to the proof of Theorem 2, it can be concluded that Theorem 3 is established.

One advantage of the FCDO is that it does not require any information about the disturbance in advance, and there is not any restriction on the first derivative of the disturbance, which can overcome the shortcomings of the conservativeness of the general disturbance observer. Most importantly, noise of the input signal can be well suppressed and the disturbance estimation accuracy is improved. The maneuvering acceleration of the low-altitude target can be regarded as an uncertain disturbance, and thus the maneuvering acceleration A_{Tq} can be estimated by FCDO.

Because of $d = A_{Tq}/R$, thus

$$\widehat{A}_{Tq} = R\hat{d}. \tag{32}$$

Due to $\dot{\hat{x}}_1 = \hat{x}_2$, thus

$$\hat{x}_1 = x_1(0) + \hat{x}_2 \Delta t, \tag{33}$$

where $x_1(0)$ is the initial value of x_1 and Δt denotes the time interval. □

5. CNFTSM Guidance Law Designed Based on FCDO

Assuming that the target acceleration estimation error satisfies $|A_{Tq} - \widehat{A}_{Tq}| \leq \varphi$, to effectively suppress measurement noise in the NFTSM guidance law, then the estimated value of FCDO and the sign function with switch coefficient ε sign(S) are introduced into the NFTSM guidance law shown as (14) to obtain the CNFTSM guidance law as follows:

$$A_{MC} = \frac{\left(-2\dot{R}\hat{x}_2 + \widehat{A}_{Tq} + \varepsilon \operatorname{sign}(S) + R\left(h_1\hat{x}_2 + h_2\dot{g}(\hat{x}_1) + k_1 S + k_2 sig(S)^{\alpha_1}\right)\right)}{\cos(\hat{x}_1 + q_d - \theta_M)}. \tag{34}$$

Theorem 4. *When the switch coefficient of the sign function satisfies $\varepsilon > \varphi$, the guidance law shown as (34) can ensure that the LOS angle converges to the desired angle within a limited time and the LOS angular rate converges to a small neighborhood near zero.*

Proof. Considering the stage of approaching the sliding surface, the Lyapunov function is selected as

$$V_1 = \frac{1}{2}S^2. \tag{35}$$

Differentiating (35) gives

$$\begin{aligned}
\dot{V}_1 &= S\dot{S} \\
&\approx \frac{S}{R}\left(A_{Tq} - \widehat{A}_{Tq} - \varepsilon \operatorname{sign}(S)\right) \\
&\quad + S\left(-k_1 S - k_2 sig(S)^{\alpha_1}\right) \\
&\leq \frac{|S|}{R}(\varphi - \varepsilon) - k_1 S^2 - k_2 |S|^{\alpha_1 + 1} \\
&\leq -k_1 S^2 - k_2 |S|^{\alpha_1 + 1} \\
&= -2k_1 V_1 - \left(\sqrt{2}\right)^{\alpha_1 + 1} k_2 V_1^{(\alpha_1 + 1)/2}.
\end{aligned} \tag{36}$$

From Lemma 1, we can see that the sliding surface can be reached by the system state in finite time.

In the stage of moving along the sliding surface, when $|x_1| > \xi$, it can be obtained that

$$S = x_2 + h_1 x_1 + h_2 sig(x_1)^{\alpha} = 0. \tag{37}$$

Select the Lyapunov function as

$$V_2 = \frac{1}{2}{x_1}^2. \tag{38}$$

Differentiating (38) gives

$$\begin{aligned}
\dot{V}_2 &= x_1\dot{x}_1 = x_1\left(-h_1 x_1 - h_2 sig(x_1)^{\alpha}\right) \\
&= -h_1 {x_1}^2 - h_2 |x_1|^{\alpha + 1} \\
&= -2h_1 V_2 - \left(\sqrt{2}\right)^{\alpha + 1} h_2 V_2^{(\alpha + 1)/2}.
\end{aligned} \tag{39}$$

From Lemma 1, it can be seen that the state variable x_1 can converge into the region $|x_1| \leq \xi$ within a limited time. Meanwhile, according to (37), the other state variable x_2 satisfies

$$|x_2| \leq h_1 |x_1| + h_2 |x_1|^{\alpha} \leq h_1 \xi + h_2 \xi^{\alpha}. \tag{40}$$

Similarly, when $|x_1| \leq \xi$, it can be obtained that

$$S = x_2 + h_1 x_1 + h_2\left(m_1 x_1 + m_2 \operatorname{sign}(x_1) {x_1}^2\right) = 0. \tag{41}$$

which implies that

$$\begin{aligned}
|x_2| &\leq h_1 |x_1| + h_2 \left|m_1 x_1 + m_2 \operatorname{sign}(x_1) {x_1}^2\right| \\
&\leq h_1 \xi + h_2 \xi^{\alpha}.
\end{aligned} \tag{42}$$

In summary, it can be concluded that the guidance law shown as (34) can ensure that the state variables of the system converge into the following region within a limited time.

$$\begin{aligned} |x_1| &\le \xi \\ |x_2| &\le h_1\xi + h_2\xi^{\alpha}. \end{aligned} \tag{43}$$

□

Equation (43) indicates that, by adjusting the value of the parameter ξ, the final convergence accuracy of the state variables x_1 and x_2 can be controlled. The smaller the parameter ξ is, the higher the convergence accuracy is. When ξ is small enough, the state variables will converge into a quite small neighborhood near zero; i.e., the LOS angle can converge to the desired angle.

6. Simulation and Discussion

Case 1 (verification of FCD performance). To verify the estimation performance of the designed FCD, a comparison between FCD and the following TD is carried out

TD: [21]

$$\begin{aligned} \dot{z}_1 &= z_2 \\ \dot{z}_2 &= \lambda^2\left[v(t) - z_1 - \frac{z_2}{\lambda}\right], \end{aligned} \tag{44}$$

where $v(t) \in \mathbf{R}$ is the input signal, $\lambda \in \mathbf{R}^+$ is the parameter to be designed, and z_1 and z_2 are the estimated values of $v(t)$ and $\dot{v}(t)$, respectively.

Take the input signal $v(t) = \sin(\pi t) + \omega$, where the measurement noise ω is Gaussian white noise with a mean of 0 and a variance of 0.2; the saturation function is generally defined as $\mathrm{sat}(\cdot) = \cdot/(|\cdot| + \delta)$, where δ is a small positive constant; let $\delta = 0.1$; the parameters of TD and FCD are chosen as $\lambda = 200$, $c_1 = 0.02$, and $c_2 = 0.05$. And the simulation results are shown in Figure 2.

As can be seen from Figure 2(a), the hyperbolic tangent function $\tanh(\cdot)$ has better smooth switching characteristics near the zero point than the saturation function $\mathrm{sat}(\cdot)$, where high-frequency chattering of the output can be more effectively suppressed and this is also the reason for constructing the FCD with the hyperbolic tangent function instead of saturation function. Figures 2(b), 2(c), and 2(d) show that the input signal with noise can be effectively tracked by the FCD designed based on the hyperbolic tangent function, whose ability to suppress the noise is stronger than TD as well. More importantly, the first derivative of the input signal can be estimated by FCD more smoothly and accurately when the measurement noise is a bit large, while TD is poor in estimation performance on the first derivative of the input signal.

Case 2 (the interception performance of NFTSM and CNFTSM guidance law). In order to verify the excellent interception and noise suppressing performance of the CNFTSM guidance law designed based on FCDO, it is compared with the NFTSM guidance law without disturbance observer designed as (14).

The energy consumption during the interception process is related to the acceleration response of the interceptor, and the average energy consumption during the interception process can be defined as

$$E = \frac{1}{n}\sum_{i=1}^{n}|A_M|, \tag{45}$$

where n denotes the total number of iterations in the simulation.

Parameters of the target and the interceptor are set as follows. The initial position coordinates of the target are $Y_T = 10\,\mathrm{m}$ and $X_T = 7800\,\mathrm{m}$, the velocity of the target is $V_T = 200\,\mathrm{m/s}$, and its initial flight path angle is $\theta_T = 180^\circ$; the initial position coordinates of the interceptor are $X_M = 0\,\mathrm{m}$ and $Y_M = 3500\,\mathrm{m}$, the velocity of the interceptor is $V_M = 400\,\mathrm{m/s}$, its initial flight path angle is $\theta_M = -45^\circ$, and the desired terminal LOS angle is $q_d = -30^\circ$, where parameters of guidance laws are chosen as $h_1 = 0.2$, $h_2 = 0.2$, $\alpha = 0.6$, $\varepsilon = 5$, $k_1 = 10$, $k_2 = 15$, $\alpha_1 = 0.5$, and $\xi = 0.01$; the parameters of FCDO are designed as $\lambda = 300$, $c_1 = 0.001$, and $c_2 = 0.017$; assume that the measurement noise ω of the LOS angular rate is Gaussian white noise with a mean of 0 and a variance of 1.5×10^{-3}. And the maneuvering acceleration of the target is set as $A_T = -20\sin(0.5\pi t)$.

The blind spot for the seeker is set as $R_b = 300\,\mathrm{m}$ and the effective lethal radius of the interceptor is set as $r_m = 3\,\mathrm{m}$ based on real engineering applications. The guidance command of the interceptor will become zero when the seeker enters the blind spot, and the interceptor continues to fly by inertia until it hits the target. Meanwhile, due to the limitation of the physical structure, the maximum acceleration response of the interceptor is assumed as $20g$, where $g \approx 9.8\,\mathrm{m/s^2}$ is the gravitational acceleration. The simulation results of the interception performance are shown in Figure 3 and Table 1.

As can be seen from Figures 3(c), 3(d), and 3(e), when intercepting a low-altitude target, the NFTSM guidance law will be affected by the measurement noise of the LOS angular rate, which will dramatically reduce the interception accuracy and result in the acceleration response of the interceptor being in the switching state between two limit values. In the actual project, it is a huge challenge to the performance of the actuator, and it may even lead to a failure of the power system. Meanwhile, it can be seen from Figure 3(a) that the interception trajectory of the NFTSM guidance law has a quite large deviation from the ideal interception trajectory. Table 1 shows some poor performance of the NFTSM guidance law in intercepting the low-altitude target in the main following two aspects. Firstly, the terminal miss distance reaches 4.19 m, which is beyond the effective killing radius of the interceptor, so that the low-altitude target cannot be effectively intercepted. Secondly, the average energy consumed in the entire interception process is as high as 15.54 g, accounting for 77.7% of the maximum amplitude of

Table 1: Comparison of two guidance laws.

Guidance law	Miss distance /m	Average energy consumption/g
NFTSM	4.19	15.54
CNFTSM	2.08	6.55

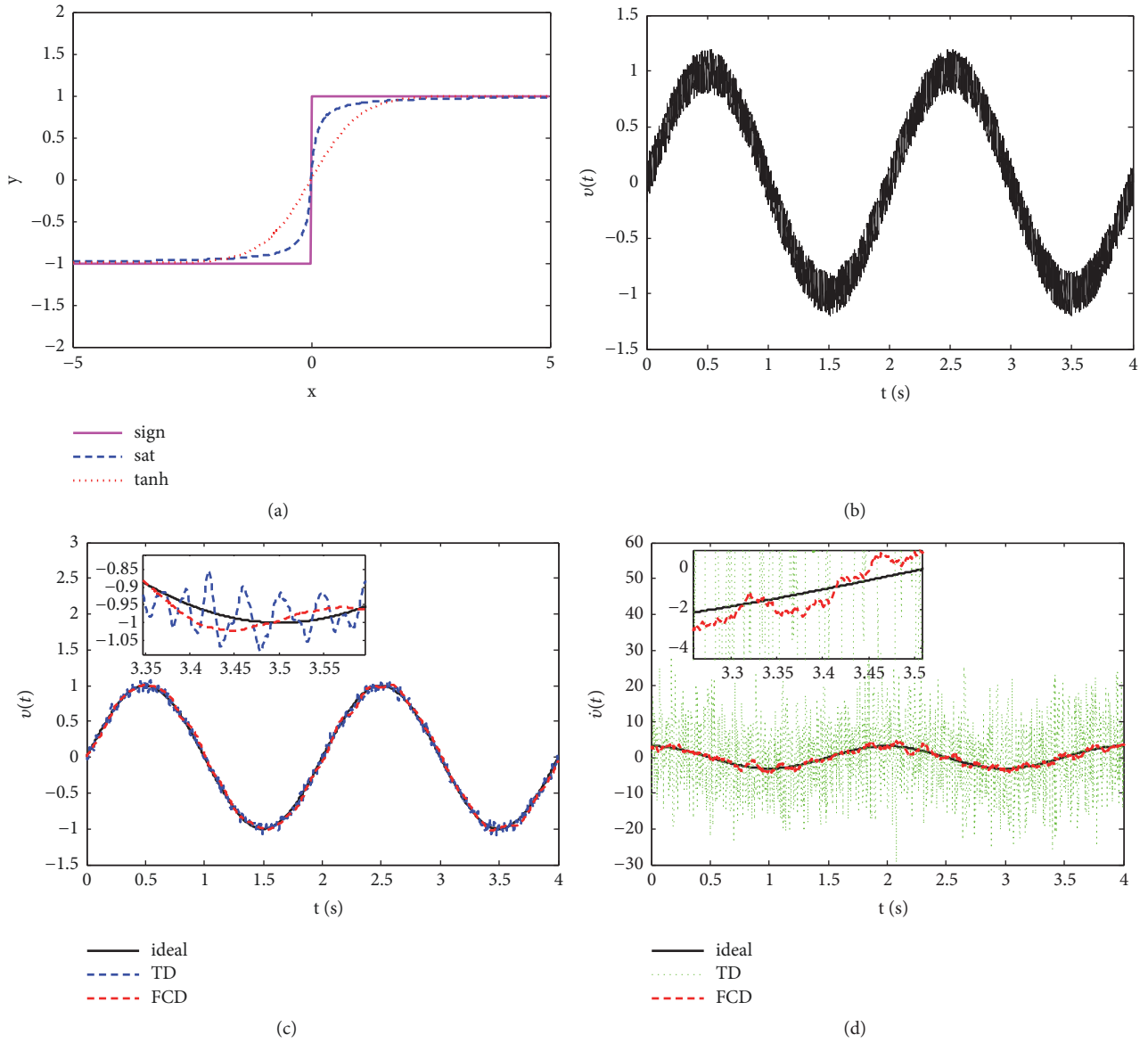

Figure 2: Simulation results for two differentiators: (a) comparison between tanh(·), sat(·), and sign function; (b) input signal $v(t)$ with noise; (c) tracking value of $v(t)$; (d) estimated value of $\dot{v}(t)$.

the acceleration response. This is an astonishing consumption ratio, which will dramatically limit the interceptor's flight distance so that its engineering application is greatly limited.

However, compared with NFTSM guidance law, it can be seen from Figures 3(c), 3(d), 3(e), and 3(f) that the CNFTSM guidance law can effectively suppress the measurement noise of the LOS angular rate due to the introduction of the estimated values of FCDO and can further make a smooth estimation of the target acceleration, which can improve the interception accuracy and ensure that the interceptor effectively intercepts the low-altitude target with an approximately ideal trajectory shown in Figure 3(a). Meanwhile, as can be seen from Table 1, the terminal miss distance of the CNFTSM guidance law is only 2.08 m, within the effective lethal radius of the interceptor and so the interceptor can successfully intercept and hit the low-altitude target. Moreover, the average energy consumed during the entire interception process is only 6.55 g, accounting for

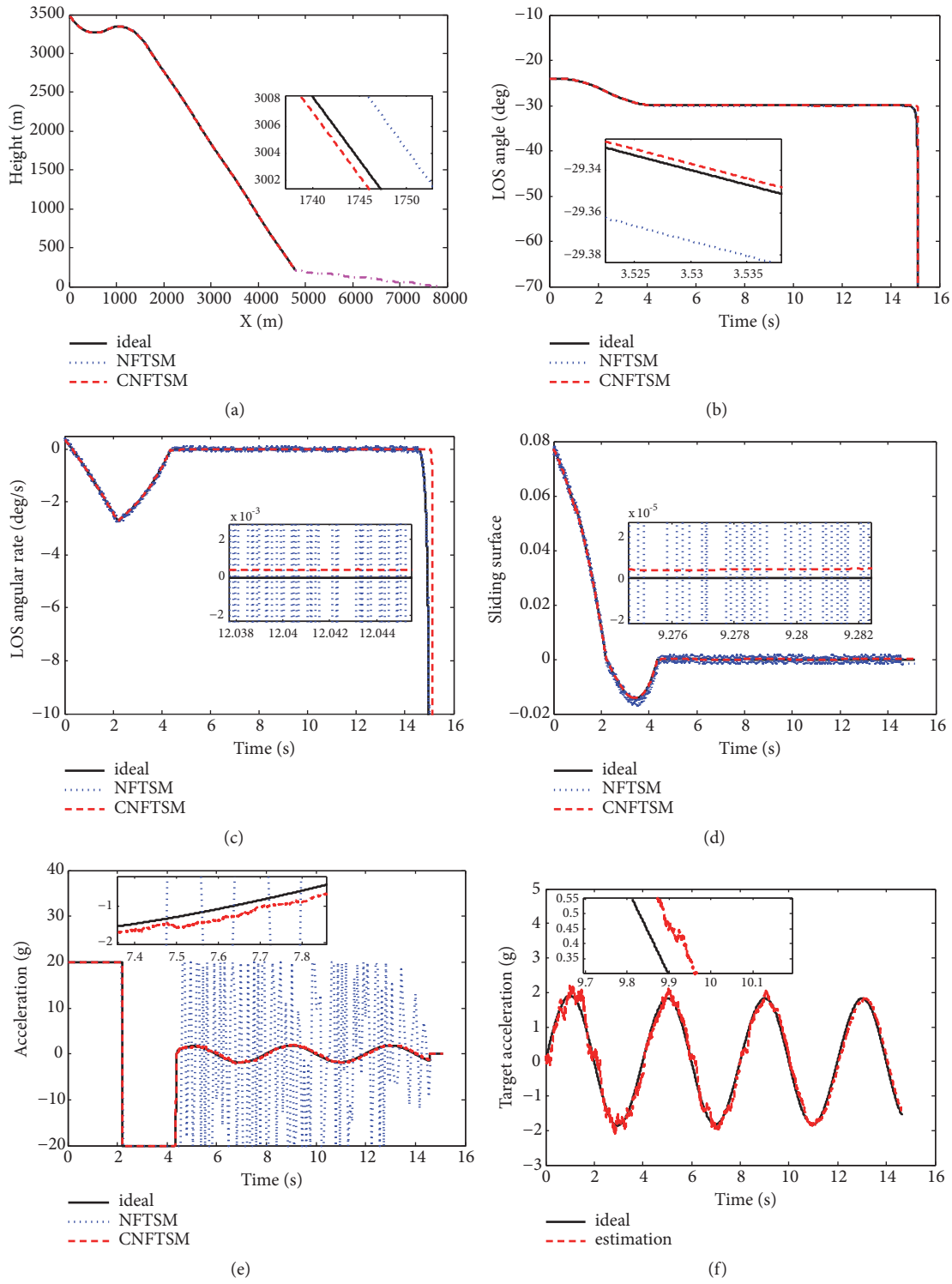

FIGURE 3: Simulation results for Case 2: (a) interception trajectory; (b) LOS angle; (c) LOS angular rate; (d) sliding surface; (e) acceleration response of interceptor; (f) estimation of target acceleration A_{Tq}.

only 32.8% of the maximum amplitude of the acceleration response, so that the interception accuracy can be greatly improved and the energy consumption can be obviously reduced. Therefore, it has a prospective engineering applicability.

7. Conclusions

To track and intercept a low-altitude target more effectively, a NFTSM guidance law with fast response characteristics is designed to quickly constrain the LOS angle to a desired angle

within a limited time, 4s. To solve the problem that guidance accuracy reduction and energy loss aggravation caused by measurement noise of the LOS angular rate in the clutter environment, the FCDO is designed to effectively suppress measurement noise of the LOS angular rate and make a smooth estimation of the target's maneuvering acceleration without any prior information about the acceleration. Finally, a CNFTSM guidance law is designed based on FCDO by introducing the estimated values of FCDO and the sign function with switch coefficient, which can effectively suppress measurement noise, reduce the miss distance from 4.19 m to 2.08 m at the end of interception compared with NFTSM guidance law, and greatly improve the interception accuracy. Most importantly, the consumption ratio of energy during the interception process can be greatly reduced from 77.7% to 32.8% compared with NFTSM guidance law. Therefore, the designed CNFTSM guidance law has wider engineering application prospect.

Appendix

Notations

η_M: A time-varying angle defined as $\eta_M = q - \theta_M$
η_T: A time-varying angle defined as $\eta_T = q - \theta_T$
V_M, V_T: Velocities of the interceptor and target
θ_M, θ_T: Flight path angles of the interceptor and target
$\dot{\theta}_M, \dot{\theta}_T$: Flight path angular rates of the interceptor and target
$R, \dot{R}$: Relative range and range rate between the interceptor and target
A_M, A_T: Acceleration command of the interceptor and target
A_{Mq}: Acceleration of the interceptor normal to the LOS
A_{Tq}: Acceleration of the target normal to the LOS
$q, \dot{q}$: LOS angle and its rate
q_d: The desired LOS angle
$\upsilon(t), \dot{\upsilon}(t)$: Input signal and its first derivative
$\hat{x}_2, \hat{d}$: Estimated values of FCDO
E: Average energy consumption
ω: Measurement noise
g: Gravitational acceleration.

Data Availability

All the conclusions of this paper are obtained with the MATLAB simulation, and the simulation parameters were pointed out in the paper and are available from the corresponding author upon request.

Conflicts of Interest

The authors declare that there are no conflicts of interest regarding the publication of this paper.

Acknowledgments

This work was supported by the National Natural Science Foundation of China (grant number 61703424).

References

[1] X. Jin, "Fault tolerant finite-time leader-follower formation control for autonomous surface vessels with LOS range and angle constraints," *Automatica*, vol. 68, pp. 228–236, 2016.

[2] X. Wang, Y. Zhang, and H. Wu, "Sliding mode control based impact angle control guidance considering the seekers field-of-view constraint," *ISA Transactions®*, vol. 61, pp. 49–59, 2015.

[3] B.-G. Park, T.-H. Kim, and M.-J. Tahk, "Optimal impact angle control guidance law considering the seeker's field-of-view limits," *Proceedings of the Institution of Mechanical Engineers, Part G: Journal of Aerospace Engineering*, vol. 227, no. 8, pp. 1347–1364, 2013.

[4] W. Chen, "Spatial and temporal features selection for low-altitude target detection," *Aerospace Science and Technology*, vol. 40, pp. 171–180, 2015.

[5] Y.-L. Qin and Y.-Q. Cheng, "Dynamic multipath model of low angle passive radar tracking with experimental evaluation," *Defence Science Journal*, vol. 62, no. 5, pp. 331–337, 2012.

[6] C. H. Lee, T. H. Kim, and M. J. Tahk, "Interception angle control guidance using proportional navigation with error feedback," *Journal of Guidance Control & Dynamics*, vol. 36, no. 5, pp. 1556–1561, 2013.

[7] R. Bardhan and D. Ghose, "Nonlinear differential games-based impact-angle-constrained guidance law," *Journal of Guidance, Control, and Dynamics*, vol. 38, no. 3, pp. 384–402, 2015.

[8] W. Yu, W. Chen, L. Yang, X. Liu, and H. Zhou, "Optimal terminal guidance for exoatmospheric interception," *Chinese Journal of Aeronautics*, vol. 29, no. 4, pp. 1052–1064, 2016.

[9] C. Guo and X.-G. Liang, "Integrated guidance and control based on block backstepping sliding mode and dynamic control allocation," *Proceedings of the Institution of Mechanical Engineers, Part G: Journal of Aerospace Engineering*, vol. 229, no. 9, pp. 1559–1574, 2015.

[10] D. Zhou, S. Sun, and JY. Zhou, "A discrete sliding-mode guidance law," *Journal of Dynamic Systems Measurement Control*, vol. 137, no. 2, Article ID 024501, 2014.

[11] Q. Z. Zhang, Z. B. Wang, F. Tao, and B. R. Sarker, "On-line optimization design of sliding mode guidance law with multiple constraints," *Applied Mathematical Modelling: Simulation and Computation for Engineering and Environmental Systems*, vol. 37, no. 14-15, pp. 7568–7587, 2013.

[12] P. Skruch, "A Terminal Sliding Mode Control of Disturbed Nonlinear Second-Order Dynamical Systems," *Journal of Computational and Nonlinear Dynamics*, vol. 11, no. 5, 2016.

[13] D. Cho, H. J. Kim, and M.-J. Tahk, "Nonsingular sliding mode guidance for impact time control," *Journal of Guidance, Control, and Dynamics*, vol. 39, no. 1, pp. 61–68, 2016.

[14] N. Boonsatit and C. Pukdeboon, "Adaptive Fast Terminal Sliding Mode Control of Magnetic Levitation System," *Journal of Control, Automation and Electrical Systems*, vol. 27, no. 4, pp. 359–367, 2016.

[15] J. Zhu, L. Liu, G. Tang, and W. Bao, "Three-dimensional robust diving guidance for hypersonic vehicle," *Advances in Space Research*, vol. 57, no. 2, pp. 562–575, 2016.

[16] S. Ghosh, S. Mukhopadhyay, and A. Routray, "New state and measurement models for endo-atmospheric tracking of ballistic targets using seeker measurements," *IEEE Transactions on Aerospace and Electronic Systems*, vol. 48, no. 2, pp. 1192–1209, 2012.

[17] J. Zhao, D.-J. Feng, and W. Wang, "Augmenting inertial navigation system with radar seeker mainlobe clutter tracking," in *Proceedings of the 2012 2nd IEEE International Conference on Signal Processing, Communications and Computing, ICSPCC 2012*, pp. 640–643, China, August 2012.

[18] Z. Wang and Z. Wu, "Nonlinear attitude control scheme with disturbance observer for flexible spacecrafts," *Nonlinear Dynamics*, vol. 81, no. 1-2, pp. 257–264, 2015.

[19] B. Xu, Z. K. Shi, and C. G. Yang, "Composite fuzzy control of a class of uncertain nonlinear systems with disturbance observer," *Nonlinear Dynamics*, 2015.

[20] J. Han, H. Zhang, Y. Wang, and Y. Liu, "Disturbance observer based fault estimation and dynamic output feedback fault tolerant control for fuzzy systems with local nonlinear models," *ISA Transactions®*, vol. 59, pp. 114–124, 2015.

[21] G. Y. Qi, Z. Q. Chen, and Z. Z. Yuan, "New tracking-differentiator design and analysis of its stability and convergence," *Journal of Systems Engineering and Electronics*, vol. 15, no. 4, pp. 780–787, 2004.

[22] F. Chen, G. J. He, and Q. F. He, "A finite-time-convergent composite guidance law with strong fault-tolerant performance," *Proceedings of the Institution of Mechanical Engineers, Part G: Journal of Aerospace Engineering*, vol. 18, no. 7, pp. 154–167, 2018.

[23] S. Yu, X. Yu, B. Shirinzadeh et al., "Continuous finite-time control for robotic manipulators with terminal sliding mode. Information Fusion," in *Proceedings of the Sixth International Conference of. IEEE 2005*, pp. 1433–1440, 2003.

[24] X. Wang, Z. Chen, and G. Yang, "Finite-time-convergent differentiator based on singular perturbation technique," *IEEE Transactions on Automatic Control*, vol. 52, no. 9, pp. 1731–1737, 2007.